Flutter Analysis of Multiple Blade Rows Vibrating Under Aerodynamic Coupling

Ayumi Kubo and Masanobu Namba
Sojo University
4-22-1, Ikeda, Kumamoto, Japan
namba@arsp.sojo-u.ac.jp

Keywords: Aeroelasticity, Axial Compressor, Flutter, Rotor-Stator Interaction

Abstract

This paper deals with the aeroelastic instability of vibrating multiple blade rows under aerodynamic coupling with each other. A model composed of three blade rows, e.g., rotor-stator-rotor, where blades of the two rotor cascades are simultaneously vibrating, is considered. The displacement of a blade vibrating under aerodynamic force is expanded in a modal series with the natural mode shape functions, and the modal amplitudes are treated as the generalized coordinates. The generalized mass matrix and the generalized stiffness matrix are formulated on the basis of the finite element concept. The generalized aerodynamic force on a vibrating blade consists of the component induced by the motion of the blade itself and those induced not only by vibrations of other blades of the same cascade but also vibrations of blades in another cascade. To evaluate the aerodynamic forces, the unsteady lifting surface theory for the model of three blade rows is applied. The so-called *k* method is applied to determine the critical flutter conditions. A numerical study has been conducted. The flutter boundaries are compared with those for a single blade row. It is shown that the effect of the aerodynamic blade row coupling substantially modifies the critical flutter conditions.

Nomenclature

$\bar{b}$ = mean semichord of a blade
C_{aj} = axial chord length of Row j : j = U, M or D
E^* = Young's modulus of blade material
$\boldsymbol{F}$ = generalized force matrix
F_{mm} = generalized aerodynamic force coefficient : Eq. (13)
G_{UM} , G_{DM} = distance between centers of blade rows: Fig 1
h = hub-to-tip ratio
$i = \sqrt{-1}$
$\boldsymbol{K}$ = generalized stiffness matrix
K_{nm} = generalized modal stiffness : Eq. (9)
M_a = axial Mach number
$\boldsymbol{M}$ = generalized mass matrix
M_{nm} = generalized modal mass : Eq. (7)
m_b^* = mass of a blade
N_j = number of blades of Row j : j = U, M or D
r = radial coordinate
r_T^* = outer radius of the annular duct: rotor tip radius
s = chordwise coordinate
t = time
W_a^* = axial flow velocity
$W_m^j(r,s)$ = natural mode shape of order m of a blade in Row j
X = frequency ratio squared : Eq. (24)
z = axial coordinate
$\Delta p_m(r,s)$ = the fundamental frequency component of pressure difference between the lower and upper surfaces of a blade caused by blade vibration of natural mode m
$\Delta p_{(\mu,\nu)}(r,s)$ = pressure difference between the lower and upper surfaces of a blade: component of harmonic number μ and ν
κ = parameter defined by Eq. (32)
λ = aspect ratio of a blade : Eq. (30)
μ = mass ratio of a blade : Eq. (31)
ν = Poisson's ratio of blade material
ρ_0^* = mass density of air
ρ_b^* = mass per unit surface area of a blade
σ = number of nodal diameters in the traveling wave mode of blade row vibration: interblade phase angle × number of blades / 2π
$\tau^*(r,s)$ = blade thickness
Ω = angular velocity
ω = reduced frequency (= $\omega^* r_T^* / W_a^*$)
ω_B^* = natural frequency of the first bending mode of a cantilever thin plate
ω_F^* = critical flutter frequency

Subscripts or superscripts
U = Row U (the upstream blade row)
M = Row D (the middle blade row)
D = Row D (the downstream blade row)

1. Introduction

The key factors governing the aerelastic instability called flutter are inertia forces, elastic forces, and aerodynamic forces induced by vibrating motions of

the structural elements. In particular, we should note that a vibrating motion of a blade in a turbomachine gives rise to aerodynamic forces not only on the vibrating blade itself but also on other blades in the turbomachine. Therefore the essential feature of the cascade flutter is the mutual interaction of blades under aerodynamic coupling.

In this respect, it should be noticed that the actual turbomachines are in general composed of multiple blade rows which are closely placed. Therefore it is reasonably expected that the aerodynamic interaction between the blade rows will give a substantial influence on the cascade flutter.

It is, however, since 1990's that the models on which the cascade flutter problem is studied have been expanded from a single blade row to multiple blade rows.

It is rather a limited number of researchers that have studied the problems related to the flutter of multiple blade rows so far. Hall and his colleagues have developed a two-dimensional cascade theory1) and three-dimensional CFD Euler solvers2-4) to calculate the unsteady aerodynamic forces on oscillating blades in multiple blade rows. On the other hand, Namba and his colleagues5-6) have developed a lifting surface theory for oscillating blades in a contra-rotating blade rows.

Most of the previous researches1- 6), however, are confined to study of the influence of neighboring blade rows on unsteady aerodynamic response of oscillating blades, and do not extend the study to the aeroelastic instability analysis including the influence of neighboring blade rows.

As far as we are aware, Namba and Nishino's paper7) is only one published work solving the problem of the aeroelastic instability of multiple blade rows. They conducted the flutter analysis of contra-rotating blade rows, and indicated that the presence of a neighboring blade row brings about significant modifications to the flutter boundaries.

In that paper, however, they assume that only blades of one of the two rows are vibrating and those of the other blade row are stationary. Therefore the problem of mutual aerodynamic excitation of vibrating two blade rows is not dealt with. One of the reasons that they dealt with such a model is clear. In case of two blade rows in a mutual rotational motion, oscillations of blades in one of the two blade rows induce unsteady aerodynamic forces on blades of the counter blade row with frequencies equal to the blade vibration frequency plus the rotational angular speed multiplied by circumferential wave numbers of the traveling wave mode of the blade row oscillation. Therefore if the elastic properties of both blade rows are similar, as is usually the case, the instability of blade vibrations caused by mutual aerodynamic excitation of the two adjacent blade rows is unlikely to occur.

Recently, Namba et al.8) developed an unsteady lifting surface theory for a model of three blade rows and conducted unsteady aerodynamic analyses assuming blades of one of the three blade rows are oscillating. As one of the important findings from their study, it is pointed out that the oscillation of blades brings about unsteady aerodynamic forces of considerable magnitude even on blades of the next blade row but one. This implies that the instability of blade vibration caused by mutual aerodynamic excitation of the two co-rotating or stationary blade rows placed next but one is likely to occur.

The purpose of this paper is to conduct the flutter analysis of a model of three blade rows in which two of the three blade rows are vibrating at a common frequency under aerodynamic coupling, and make clear the difference in the flutter conditions between the isolated blade row and the aerodynamically coupled multiple blade rows.

2. Mathematical Formulation

2.1 Model Description

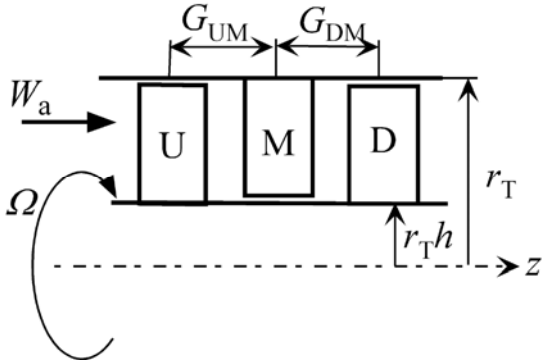

Figure 1. Model of Rotor U/Stator M/Rotor D.

We consider a model of three blade rows in an annular duct with the outer duct radius r_T^* and the boss ratio h as shown in Fig. 1. The undisturbed flow is a uniform axial flow of axial velocity W_a^*, fluid density ρ_0^*, and axial Mach number M_a. In the following, unstarred symbols denote dimensionless quantities, where lengths, velocities, pressures, and times are scaled with respect to r_T^*, W_a^*, $\rho_0^* W_a^{*2}$, and r_T^* / W_a^*, respectively. We denote the upstream, middle, and downstream cascades by Row U, Row M, and Row D, respectively, and use subscripts or superscripts U, M, and D to identify the blade rows. Let the angular velocity of Row U and Row D be $\Omega\left(=\Omega^* r_T^* / W_a^*\right)$, the numbers of blades be N_U, N_M, N_D, and the axial chord lengths of blades (constant along the span) be C_{aU}, C_{aM}, and C_{aD}. We assume that the disturbances are small. Therefore the governing equations are linearized.

2.2 Nature of Unsteady Aerodynamic Force

Assume that the blades of Row U and Row D are making simple harmonic vibrations with frequencies ω_U and ω_D, and interblade phase angles $2\pi\sigma_U / N_U$ and $2\pi\sigma_D / N_D$, respectively. Here, σ_U and σ_D are

integers between $-N_U/2$ and $N_U/2$, and between $-N_D/2$ and $N_D/2$, respectively. Then, the blade loading (pressure difference between the upper and lower surfaces of a blade) caused by vibrations of the blades under aerodynamic coupling among the blade rows can be expressed as follows[8]:

Row U : m -th blade ($m = 0,1,2,\cdots,N_U-1$)

$$\Delta p^{(U)}(r,s,t) = \sum_{\nu=-\infty}^{\infty}\sum_{\lambda=-\infty}^{\infty}\Big[\Delta p_{(\nu,\lambda)}^{(U-U)}(r,s) \times e^{i(\omega_U-\nu N_M\Omega)t+i2\pi(\sigma_U+\nu N_M+\lambda N_D)m/N_U} + \Delta p_{(\nu,\lambda)}^{(U-D)}(r,s) \times e^{i(\omega_D-\nu N_M\Omega)t+i2\pi(\sigma_D+\nu N_M+\lambda N_D)m/N_U}\Big] \quad (1)$$

Row M : m -th blade ($m = 0,1,2,\cdots,N_M-1$)

$$\Delta p^{(M)}(r,s,t) = \sum_{\nu=-\infty}^{\infty}\sum_{\lambda=-\infty}^{\infty}\Big[\Delta p_{(\lambda,\mu)}^{(M-U)}(r,s) \times e^{i(\omega_U+\{\mu N_U+\sigma_U+\lambda N_D\}\Omega)t+i2\pi(\sigma_U+\mu N_U+\lambda N_D)m/N_M} + \Delta p_{(\lambda,\mu)}^{(M-D)}(r,s) \times e^{i(\omega_D+\{\mu N_U+\sigma_U+\lambda N_D\}\Omega)t+i2\pi(\sigma_D+\mu N_U+\lambda N_D)m/N_M}\Big] \quad (2)$$

Row D : m -th blade ($m = 0,1,2,\cdots,N_D-1$)

$$\Delta p^{(U)}(r,s,t) = \sum_{\mu=-\infty}^{\infty}\sum_{\nu=-\infty}^{\infty}\Big[\Delta p_{(\mu,\nu)}^{(D-D)}(r,s) \times e^{i(\omega_D-\nu N_M\Omega)t+i2\pi(\sigma_D+\nu N_M+\mu N_U)m/N_D} + \Delta p_{(\mu,\nu)}^{(D-U)}(r,s) \times e^{i(\omega_U-\nu N_M\Omega)t+i2\pi(\sigma_U+\nu N_M+\mu N_U)m/N_D}\Big] \quad (3)$$

Here, $\Delta p_{(\nu,\lambda)}^{(U-D)}(r,s)$ implies the aerodynamic force on Row U caused by vibration of Row D. Further, r denotes the radial (spanwise) coordinate and s denotes the chordwise coordinate. We should note that the aerodynamic forces on the blades are composed of an infinite number of frequency components. The components are identified by integral numbers ν, λ and μ.

It is pointed out by Nakagawa and Namba[8] that the components other than the lowest frequency component ($\nu = \lambda = \mu = 0$) are in general very small. We should note further that the vibrating motions of blade rows can be excited or damped by the component of the aerodynamic force of the same frequency and the same interblade phase angle as those of the blade row vibration. Therefore in order for mutual excitation of vibrations via aerodynamic coupling to occur between Row U and Row D, it is necessary that $\omega_U = \omega_D$ and $\sigma_U = \sigma_D$. Consequently in the following flutter analysis, we assume Row U and Row D are vibrating at a common frequency ω and with a common number of nodal diameters σ.

Further we take only the aerodynamic force of the lowest frequency component $\Delta p_{(0,0)}(r,s)$ into account.

2.3 Equations of Motion of Blades

We express the unsteady displacement of a blade normal to the blade surface as follows.

$$w^U(r,s,t) = \sum_{m=1}^{\infty} W_m^U(r,s) w_m^U(t) \quad (4)$$

$$w^D(r,s,t) = \sum_{m=1}^{\infty} W_m^D(r,s) w_m^D(t) \quad (5)$$

Here, $W_m^U(r,s)$ and $W_m^D(r,s)$ denote mode shape functions, i.e., displacement shapes of natural free vibration of the blade of mode m. Then unknown functions of time $w_m^U(t)$ and $w_m^D(t)$ are generalized coordinates in the formulation of Lagrange's equations.

Kinetic Energy

The kinetic energy of the blade motion is written as

$$T = \frac{1}{2}\sum_m\sum_n\left\{M_{nm}^U \dot{w}_n^U \dot{w}_m^U + M_{nm}^D \dot{w}_n^D \dot{w}_m^D\right\} \quad (6)$$

where M_{nm}^U and M_{nm}^D are generalized modal masses :

$$M_{nm} = \iint_{\text{blade surface}} \rho_b^*(r,s) W_n(r,s) W_m(r,s) dr ds \quad (7)$$

Here $\rho_b^*(r,s)$ denote mass per unit surface area of a blade.

Potential Elastic (Strain) Energy

In this paper, we assume that blades are thin, so that the strain energy is written as

$$U = \frac{1}{2}\sum_n\sum_m (K_{nm}^U w_n^U w_m^U + K_{nm}^D w_n^D w_m^D) \quad (8)$$

where K_{nm}^U and K_{nm}^D are generalized modal masses:

$$K_{nm} = \iint_{\text{blade surface}} D^*\left[\frac{\partial^2 W_m}{\partial s^2}\left(\frac{\partial^2 W_n}{\partial s^2} + \nu\frac{\partial^2 W_n}{\partial r^2}\right) + \frac{\partial^2 W_m}{\partial r^2}\left(\frac{\partial^2 W_n}{\partial r^2} + \nu\frac{\partial^2 W_n}{\partial s^2}\right) + 2(1-\nu)\frac{\partial^2 W_m}{\partial r \partial r}\frac{\partial^2 W_n}{\partial r \partial r}\right] dr ds \quad (9)$$

Further, $$D^* = \frac{E^*}{12(1-\nu^2)}\left\{\tau^*(r,s)\right\}^3 \quad (10)$$

E^* is Young's modulus, ν is Poisson's ratio, and τ^* is thickness of a blade.

Generalized Force

The virtual work caused by virtual displacements δw_n^U and δw_n^D $(n = 1,2,\cdots)$ can be written as

$$\delta W = \sum_n\left\{\delta w_n^U(t) F_n^U(t) + \delta w_n^D(t) F_n^D(t)\right\} \quad (11)$$

where $F_n^U(t)$ and $F_n^D(t)$ are generalized forces on the blades of Row U and Row D, respectively.

$$F_n^U(t) = \sum_m \left\{ F_{nm}^{U-U} w_m^U(t) + F_{nm}^{U-D} w_m^D(t) \right\}$$
$$F_n^D(t) = \sum_m \left\{ F_{nm}^{D-U} w_m^U(t) + F_{nm}^{D-D} w_m^D(t) \right\} \quad (12)$$

Further, the generalized force coefficients are written as

$$F_{nm}^{U-U} = \iint_{\text{surface U}} W_n^U(r,s)\Delta p_m^{U-U}(r,s)dsdr$$
$$F_{nm}^{U-D} = \iint_{\text{surface U}} W_n^U(r,s)\Delta p_m^{U-D}(r,s)dsdr$$
$$F_{nm}^{D-U} = \iint_{\text{surface D}} W_n^D(r,s)\Delta p_m^{D-U}(r,s)dsdr \quad (13)$$
$$F_{nm}^{D-D} = \iint_{\text{surface D}} W_n^D(r,s)\Delta p_m^{D-D}(r,s)dsdr$$

Here, F^{U-D} denotes generalized force on Row U caused by vibration of Row D, whereas F^{D-U} denotes generalized force on Row D caused by vibration of Row U. Further $\Delta p_m(r,s)$ denotes the fundamental frequency component of pressure difference between the lower and upper surfaces of a blade caused by blade vibration of natural mode m. In other words, $\Delta p_m(r,s)$ implies $\Delta p_{(0,0)}(r,s)$ caused by the m-th natural mode vibration of a blade.

Lagrange's Equation of Motion

Lagrange's equation of motions can be written as

$$\frac{d}{dt}\left(\frac{\partial T}{\partial \dot{w}_n^U}\right) + \frac{\partial U}{\partial w_n^U} = F_n^U : n = 1,2,\cdots$$
$$\frac{d}{dt}\left(\frac{\partial T}{\partial \dot{w}_n^D}\right) + \frac{\partial U}{\partial w_n^D} = F_n^D : n = 1,2,\cdots \quad (14)$$

Using Eqs. (6) and (8) we obtain

$$\frac{d}{dt}\left(\frac{\partial T}{\partial \dot{w}_n^U}\right) = \frac{1}{2}\sum_m M_{nm}^U \ddot{w}_m^U$$
$$\frac{d}{dt}\left(\frac{\partial T}{\partial \dot{w}_n^D}\right) = \frac{1}{2}\sum_m M_{nm}^D \ddot{w}_m^D \quad (15)$$

and

$$\frac{\partial U}{\partial w_n^U} = \frac{1}{2}\sum_m K_{nm}^U w_m^U$$
$$\frac{\partial U}{\partial w_n^U} = \frac{1}{2}\sum_m K_{nm}^D w_m^D \quad (16)$$

Then using Eqs. (15), (16) and (12), we can rewrite Eq. (14) into the form

$$\sum_m \left\{ \frac{1}{2} M_{nm}^U \ddot{w}_m^U + \frac{1}{2} K_{nm}^U w_m^U - F_{nm}^{U-U} w_m^U - F_{nm}^{U-D} w_m^U \right\} = 0$$
$$\sum_m \left\{ \frac{1}{2} M_{nm}^D \ddot{w}_m^D + \frac{1}{2} K_{nm}^D w_m^D - F_{nm}^{D-U} w_m^U - F_{nm}^{D-D} w_m^U \right\} = 0$$
$$n = 1,2,\cdots \quad (17)$$

which, we can further rewrite as follow.

$$\begin{bmatrix} (1/2)\boldsymbol{M}^U & 0 \\ 0 & (1/2)\boldsymbol{M}^D \end{bmatrix} \begin{Bmatrix} \ddot{\boldsymbol{w}}^U \\ \ddot{\boldsymbol{w}}^D \end{Bmatrix} + \begin{bmatrix} (1/2)\boldsymbol{K}^U - \boldsymbol{F}^{U-U} & -\boldsymbol{F}^{U-D} \\ -\boldsymbol{F}^{D-U} & (1/2)\boldsymbol{K}^D - \boldsymbol{F}^{D-D} \end{bmatrix} \begin{Bmatrix} \boldsymbol{w}^U \\ \boldsymbol{w}^D \end{Bmatrix} = 0 \quad (18)$$

Here, $\boldsymbol{M}$, $\boldsymbol{K}$ and $\boldsymbol{F}$ denote matrices of generalized mass, generalized stiffness and generalized force, respectively, defined as follows.

$$\boldsymbol{M} = \begin{bmatrix} M_{11} & M_{12} & \cdots \\ M_{21} & M_{22} & \\ \vdots & & \ddots \end{bmatrix}, \boldsymbol{K} = \begin{bmatrix} K_{11} & K_{12} & \cdots \\ K_{21} & K_{22} & \\ \vdots & & \ddots \end{bmatrix}$$
$$\boldsymbol{F} = \begin{bmatrix} F_{11} & F_{12} & \cdots \\ F_{21} & F_{22} & \\ \vdots & & \ddots \end{bmatrix} \quad (19)$$

and $\boldsymbol{w}$ denotes a column vector defined by

$$\boldsymbol{w} = \begin{Bmatrix} w_1 \\ w_2 \\ \vdots \end{Bmatrix} \quad (20)$$

As we can see from Eq. (17), Rotor U and Rotor D exercise influences on each other by aerodynamic forces $\boldsymbol{F}^{U\text{-}D}$ and $\boldsymbol{F}^{D\text{-}U}$

2.4 Flutter Equation

Assume that the generalized coordinates are of harmonic time dependence as follows:

$$w_n(t) = \tilde{w}_n e^{i\omega t} \quad (21)$$

Here ω is the reduced frequency defined by

$$\omega = \frac{\omega^* r_T^*}{W_a^*} \quad (22)$$

and ω^* denotes the angular frequency of blade vibration. Then we can rewrite Eq. (18) as follow:

$$\left([\boldsymbol{M}] + [\boldsymbol{F}] - X[\boldsymbol{K}] \right) \begin{Bmatrix} \tilde{\boldsymbol{w}}^U \\ \tilde{\boldsymbol{w}}^D \end{Bmatrix} = 0 \quad (23)$$

$$X = \left(\frac{\omega_B^{U*}}{\omega^*} \right)^2 \quad (24)$$

Here, $[\boldsymbol{M}]$ denotes the generalized mass matrix, $[\boldsymbol{F}]$ denotes the generalized force matrix, and $[\boldsymbol{K}]$ denotes the generalized stiffness matrix. Further, ω_B^* denotes the fundamental natural bending frequency of a thin canti-levered rectangular plate of length $r_T^*(1-h)$, thickness $\bar{\tau}^*$, Young's modulus E^* and mass density ρ_s^* given by

$$\omega_B^* = \frac{(0.597\pi)^2}{\sqrt{12}} \sqrt{\frac{E^*}{\rho_s^*}} \frac{\bar{\tau}^*}{\left\{ r_T^*(1-h) \right\}^2} \quad (25)$$

We denote ω_B^* of Row D and Row U by ω_B^{D*} and ω_B^{U*}. Therefore

$$\left(\frac{\omega_B^{D*}}{\omega_B^{U*}}\right)^2 = \left(\frac{\rho_s^{U*}}{\rho_s^{D*}}\right)\left(\frac{E^{D*}}{E^{U*}}\right)\left(\frac{\bar{\tau}^{D*}}{\bar{\tau}^{U*}}\right)^2 \tag{26}$$

The matrices of $[\boldsymbol{M}]$,$[\boldsymbol{F}]$ and $[\boldsymbol{K}]$ are defined by

$$[\boldsymbol{M}] = \begin{bmatrix} (1/2)\hat{\boldsymbol{M}}^U & 0 \\ 0 & (1/2)\hat{\boldsymbol{M}}^D \end{bmatrix} \tag{27}$$

$$[\boldsymbol{F}] = \begin{bmatrix} \dfrac{\gamma(\lambda^U)^2}{\mu^U}\dfrac{\hat{\boldsymbol{F}}^{U-U}}{\omega^2} & \dfrac{\gamma(\lambda^U)^2}{\mu^U}\dfrac{\hat{\boldsymbol{F}}^{U-D}}{\omega^2} \\ \dfrac{\gamma(\lambda^D)^2}{\mu^D}\dfrac{\hat{\boldsymbol{F}}^{D-U}}{\omega^2} & \dfrac{\gamma(\lambda^D)^2}{\mu^D}\dfrac{\hat{\boldsymbol{F}}^{D-D}}{\omega^2} \end{bmatrix} \tag{28}$$

$$[\boldsymbol{K}] = \begin{bmatrix} \lambda^U\kappa^U(1/2)\hat{\boldsymbol{K}}^U & 0 \\ 0 & \left(\dfrac{\omega_B^{D*}}{\omega_B^{U*}}\right)^2\lambda^D\kappa^D(1/2)\hat{\boldsymbol{K}}^D \end{bmatrix} \tag{29}$$

Here, λ denotes the aspect ratio of a blade

$$\lambda = \frac{r_T^*(1-h)}{C_a^*}, \tag{30}$$

μ denotes the mass ratio of a blade

$$\mu = \frac{m_b^*}{\rho_0^*\pi\bar{b}^{*2}r_T^*(1-h)}, \tag{31}$$

κ denotes

$$\kappa = \frac{(1-h)^2}{(1-\nu^2)(0.597\pi)^4}, \tag{32}$$

γ denotes

$$\gamma = \frac{4}{\pi(1-h)^3}, \tag{33}$$

m_b^* is mass of a blade and $\bar{b}$ denotes the mean semi-chord of a blade.

Equation (23) indicates that X and $\begin{bmatrix}\tilde{\boldsymbol{w}}^U & \tilde{\boldsymbol{w}}^D\end{bmatrix}^T$ are an eigenvalue and an eigenvector of matrix $[\boldsymbol{K}]^{-1}[\boldsymbol{M}+\boldsymbol{F}]$. In general, aerodynamic force $[\boldsymbol{F}]$ is complex. Therefore, eigenvalue X is complex, too.

In our flutter analysis, we search for the reduced frequency $\omega = \omega_F$ at which an eigenvalue becomes a real number. In other words put

$$X^{(m)}(\omega) = X_R^{(m)}(\omega) + iX_I^{(m)}(\omega) : m = 1,2,\cdots \tag{34}$$

and seek $\omega_F^{(m)}$ such that

$$X_I^{(m)}(\omega) = 0 \quad \text{at} \quad \omega = \omega_F^{(m)} \tag{36}$$

Then, the flutter velocity and the flutter frequency are given by

$$W_{aF}^{(m)*} = \frac{\omega_F^{(m)*}r_T^*}{\omega_F^{(m)}}, \tag{36}$$

and

$$\omega_F^{(m)*} = \frac{\omega_B^{U*}}{\sqrt{X_R^{(m)}(\omega_F^{(m)})}}, \tag{37}$$

respectively.

The corresponding flutter mode can be obtained from the eigenvector as follows:

$$w^{U(m)}(r,s,t) \propto r_T e^{i\omega_F^{(m)}t}\sum_n W_n^U(r,s)\tilde{w}_n^{U(m)} \tag{38}$$

$$w^{D(m)}(r,s,t) \propto r_T e^{i\omega_F^{(m)}t}\sum_n W_n^D(r,s)\tilde{w}_n^{D(m)} \tag{39}$$

3. Numerical Results and Discussions

3.1 Specified Condition

In this paper we deal with a combination of rotor U, stator M, and rotor D. We specify the axial Mach number $M = 0.6$, the hub-to-tip ratio $h = 0.7$ and the angular speed of rotation of the rotors $\Omega = 1.0$. The configurations of the rotors and the stator investigated are shown in Table.1.

Table 1. Specified parameters.

Configuration	1	2	3
Number of blades N_U	40	40	40
N_M	63	63	63
N_D	40	40	35
Axial chord length C_{aU}	0.1	0.1	0.1
C_{aM}	0.0794	0.0794	0.0794
C_{aD}	0.1	0.1	0.1
Mean blade thickness ratio $\bar{\tau}_U / C_{aU}$	0.04	0.04	0.04
$\bar{\tau}_D / C_{aD}$	0.04	0.045	0.04
Mass ratio μ^U	143.3	143.3	143.3
μ^D	143.3	161.2	143.3
Base frequency (rad/s) ω_B^{*U}	223.9	223.9	223.9
ω_B^{*D}	223.9	251.8	223.9
Inter- row distance $G_{UM}/(C_{aM}+C_{aU})/2$	1.1	1.1	1.1
$G_{DM}/(C_{aM}+C_{aU})/2$	1.1	1.1	1.1

In these analyses, we calculated the aerodynamic force using the unsteady lifting surface theory[8]. We computed the mode shape functions W_m^U and W_m^D using a finite element method to solve the problem of a blade vibration in a vacuum. The generalized mass matrix $\boldsymbol{M}$ and the generalized stiffness matrix $\boldsymbol{K}$ are also computed by the finite element method.

We took up to $m = 4$ in Eqs. (4) and (5). Therefore, the size of the flutter matrix is 8×8, and we obtain eight eigenvalues. Figure 2 shows the natural mode shapes functions $W_n(r,s)$ for $n = 1$ 4.

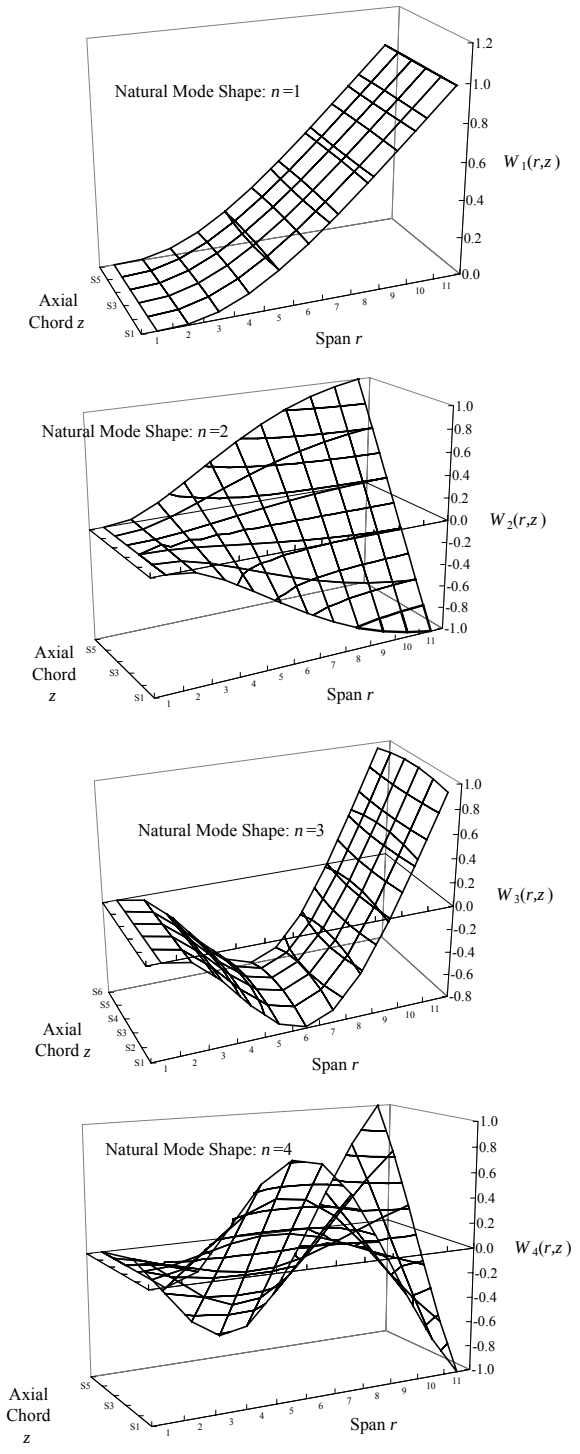

Figure 2. Natural mode shape functions.

As we can see from Fig. 2, the first natural vibration mode of the blade is similar to the first bending mode. The second natural vibration mode of the blade is similar to the first torsional mode. In the same way, the third and the fourth natural vibration modes of the blades are similar to the second bending and torsional modes, respectively.

As shown in Table 1, we consider three configurations. In Configuration 1, oscillating Row U and Row D are completely identical in the aerodynamic and elastic properties. In Configuration 2, a difference in the elastic property exists between Row U and Row D, because the blade thickness and hence the natural frequencies of Row U are different from those of Row D. We should note, however, that there is no difference in the aerodynamic property between Row U and Row D, because the lifting surface theory calculates the aerodynamic force neglecting the effect of the blade thickness. On the other hand, there is a difference in the aerodynamic property between Row U and Row D in Configuration 3, because the number of blades of Row U is different from that of Row D. But no difference exists in the elastic property.

As mentioned before, we have eight eigenvalues numbered in decreasing order of magnitude, i.e., $\left|X^{(1)}\right| \geq \left|X^{(2)}\right| \geq \cdots \geq \left|X^{(8)}\right|$. We computed the eigenvalues by increasing the reciprocal of reduced frequency ω^{-1} from a reasonably small value and searched for the value of reduced frequency $\omega = \omega_F^{(m)}$ that satisfies the condition $\mathrm{Im}\left[X^{(m)}(\omega)\right] = 0$. We found that in general one of $\omega_F^{(3)}$ and $\omega_F^{(4)}$ is the largest and the other is the second largest as demonstrated in Fig. 3. The eigenvalues other than $X^{(3)}$ and $X^{(4)}$ do not satisfy the condition up to vary high values of ω^{-1}. So we confined our attention to the two flutter conditions corresponding to $\omega_F^{(3)}$ and $\omega_F^{(4)}$. Further we call the flutter mode for the largest value of the flutter frequency given by Eq. (37) Flutter mode I, and that for the second largest value of the flutter frequency Flutter mode II.

We also computed the flutter conditions of Row U and Row D under isolated blade row conditions (no aerodynamic coupling among the blade rows).

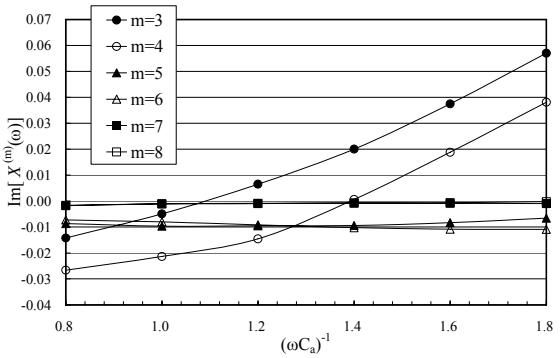

Figure 3. Variation of $\mathrm{Im}[X^{(m)}]$ with $(\omega C_a)^{-1}$. $\sigma = 8$. Configuration 1.

3.2 Flutter Frequency and Flutter Velocity

Figure 4 shows the variation of the normalized flutter frequency $\omega_F^* / \omega_B^{U*}$ with interblade phase parameter σ for Configuration 1.

In this case no difference exists in the aerodynamic and elastic properties between Row U and Row D. Therefore the flutter mode for the isolated blade row condition for Row U is identical with that for Row D.

It can be seen from Fig.4 that the flutter mode for the isolated blade row branches into two flutter

modes (Flutter mode I and Flutter mode II) by aerodynamic coupling between the blades rows. Flutter frequency of Flutter mode I is higher than that of isolated blade row, while that of Flutter mode II is lower than that of isolated blade row.

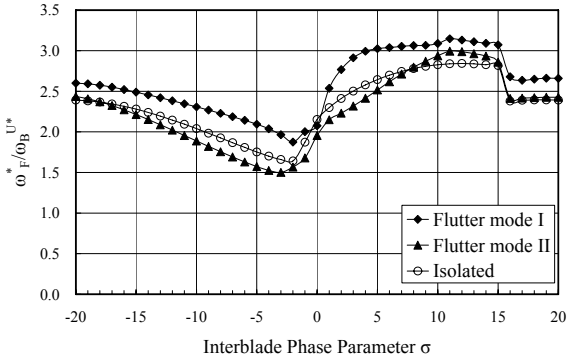

Figure 4. Normalized flutter frequency of Configuration 1.

Figures 5 and 6 show the reduced flutter frequency $\omega^*_F C^*_a / W^*_a$ and the reduced flutter velocity $W^*_{aF} / (\omega_B^{U*} C^*_a)$ for Flutter mode I, Flutter mode II and the flutter mode of the isolated blade row as functions of the interblade phase parameter σ. As shown in Fig. 5, discontinuous changes can be found in the flutter frequency across cut-off boundary of the acoustic duct mode of the lowest order.

From Figs. 5 and 6 it can be confirmed again that the flutter mode for the isolated blade row condition branches into two flutter modes. We should note that the orders of magnitude in the reduced flutter frequency (Fig. 5) and in the reduced flutter velocity (Fig. 6) are not necessarily coincident with that in the normalized flutter frequency (Fig. 4). The orders change depending on σ. However, either Flutter mode I or Flutter mode II has higher values than the isolated blade row, whereas the other has lower values than the isolated blade row except a small region of σ. In other words, the flutter velocity of either Flutter mode I or Flutter mode II is always lower than that of the isolated flutter mode, and it means that the risk of flutter occurrence is increased by aerodynamic coupling.

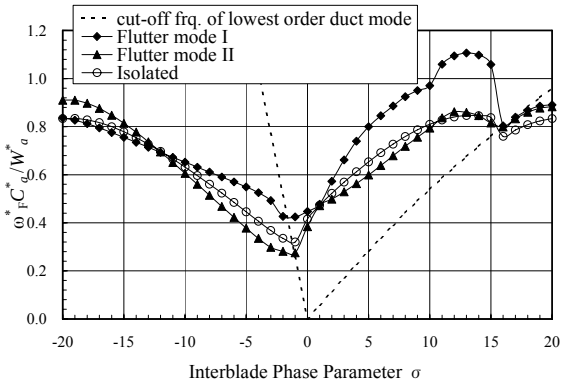

Figure 5. Reduced flutter frequency of Configuration 1. The lowest order acoustic duct mode is cut-on in the region between dash lines.

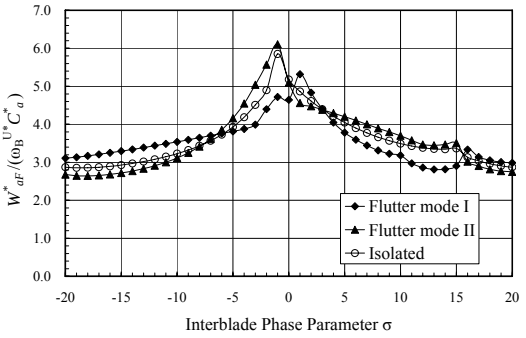

Figure 6. Reduced flutter velocity of Configuration 1.

Next, let us turn to Configuration 2. In this case the blade thickness ratio of Row D is larger than that of Row U. Consequently we have two values for the isolated Row U and the isolated Row D, and the reduced flutter velocity and the normalized flutter frequency of the isolated Row D are higher than those of the isolated Row U.

Figures 7 and 8 show the normalized flutter frequency and the reduced flutter velocity of Configuration 2. The flutter velocity of Flutter mode I is higher than that of the isolated blade row mode of Row D in almost whole region. On the other hand, the flutter velocity of Flutter mode II is lower than that of the isolated blade row mode of Row U. In contrast to Configuration 1, alternations in magnitude between the Flutter mode I and Flutter mode II do not occur except around $\sigma = -1$.

Comparing Fig. 6 with Fig. 8, we find that the lowest reduced flutter velocity of Configuration 2 (Flutter mode II) is higher than that of Configuration 1 (Flutter mode I or II). This suggests that a difference in elastic properties between Row U and Row D reduces the risk of the flutter occurrence.

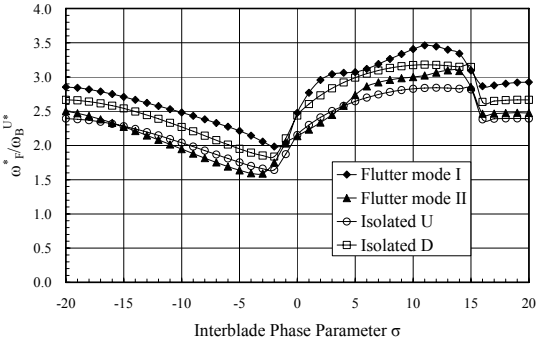

Figure 7. Normalized flutter frequency of Configuration 2.

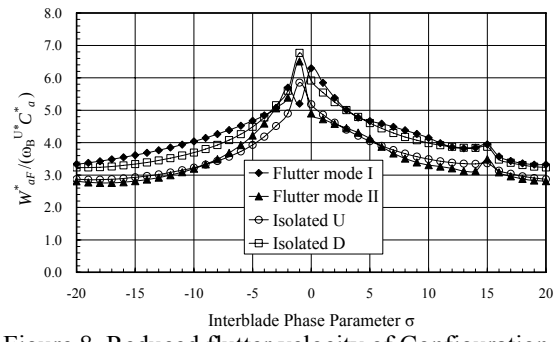

Figure 8. Reduced flutter velocity of Configuration 2.

Configuration 3 is a case that the numbers of blades of Row U and Row D are different, but Row U and Row D have same elastic property and blade shape. As we can see from Figs. 9 and 10, such a difference brings about no appreciable difference between the flutter boundary of the isolated blade Row U and that of the isolated blade Row D. Consequently, there is no essential difference also between flutter boundaries of Flutter mode I and II of Configuration 3 and those of Configuration 1.

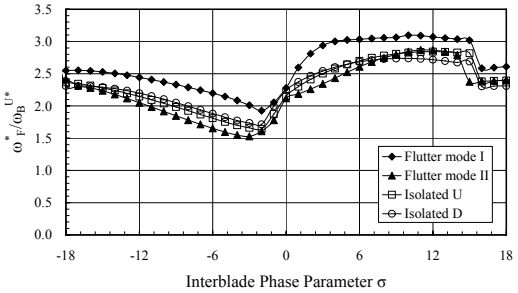

Figure 9. Normalized flutter frequency of Configuration 3.

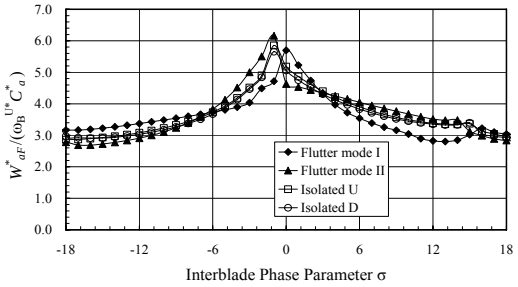

Figure 10. Reduced flutter velocity of Configuration 3.

3.3 Flutter Mode

Figure 11 shows a plot of the absolute values of the modal amplitudes of the isolated blade row flutter mode in Configuration 1 as functions of the interblade phase parameter σ. In this connection it is noteworthy that the first base mode $n=1$ and the second base mode $n=2$ are overwhelmingly dominant. Hence, the flutter modes are mainly composed of the first bending mode and first torsional mode. Furthermore, the first base mode is predominant where the lowest order duct mode is cut-off and the second base mode is predominant where the lowest order duct mode is cut-on.

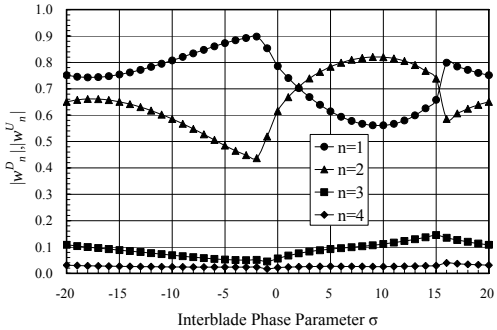

Figure 11. Absolute value of the modal amplitude of the isolated blade row flutter.

Figures 12 and 13 show absolute values of the modal amplitudes of Flutter mode I and Flutter mode II in Configuration 1, respectively. The flutter mode (Flutter mode I and Flutter mode II) influenced by the aerodynamic coupling between the blade rows also maintain the essential feature in the modal structure of the isolated blade row flutter mentioned above.

In Flutter mode I, the amplitude of Row U is much higher than that of Row D where the lowest order duct mode is cut-on, whereas the amplitude of Row D is higher than that of Row U where the lowest order duct mode is cut-off. In Flutter mode II, the amplitude of Row D is higher than that of Row U except the region of $-8 \le \sigma \le 5$.

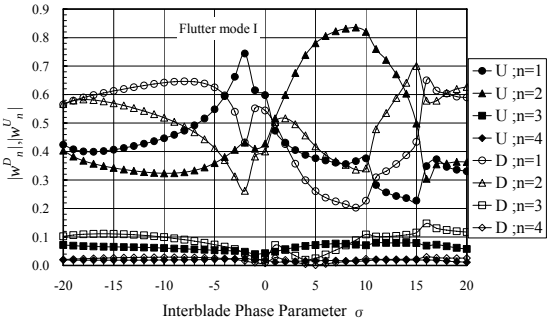

Figure 12. Absolute value of the model amplitude of Flutter mode I. Configuration 1.

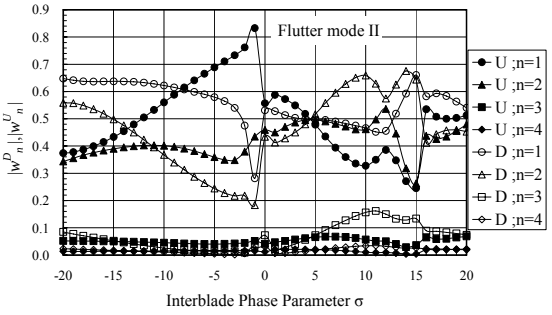

Figure 13. Absolute value of the model amplitude of Flutter mode II. Configuration 1.

Figures 14 and 15 show complex values of modal amplitudes of both blade rows in Flutter mode I and Flutter mode II at $\sigma = -15$, and Figures 16 and 17 shows those at $\sigma = 5$.

First, we can find that in general the phase of the first base mode (the first bending mode) is about 60 degrees ahead of the second base mode (the first torsion mode).

In the region where the lowest order duct mode is cut-off (Figs. 14 and 15), a motion of Row U is about 180 degrees ahead of the Row D in Flutter mode I (Fig. 15). Hence, Row U and Row D are nearly in anti-phase. On the other hand, in Flutter mode II, Row U and Row D are nearly in phase (Fig. 15) .

In the region where the lowest order duct mode is cut-on (Figs. 16 and 17), the motion of Row D is about 90□ 120 degrees ahead of the Row U in Flutter mode I (Fig. 16), whereas the converse of the

relationship between Row U and Row D is seen in Flutter mode II (Fig. 17).

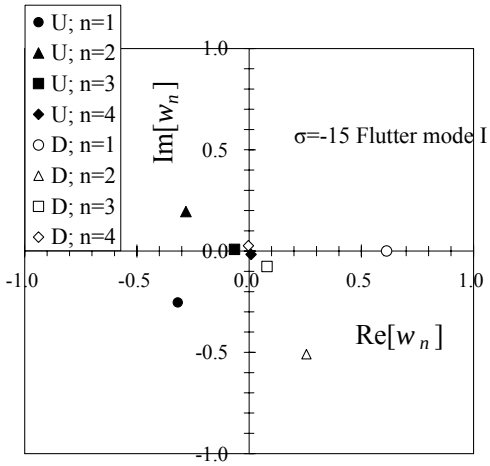

Figure 14. Complex values of the modal amplitudes of Flutter mode I at $\sigma = -15$. Configuration 1.

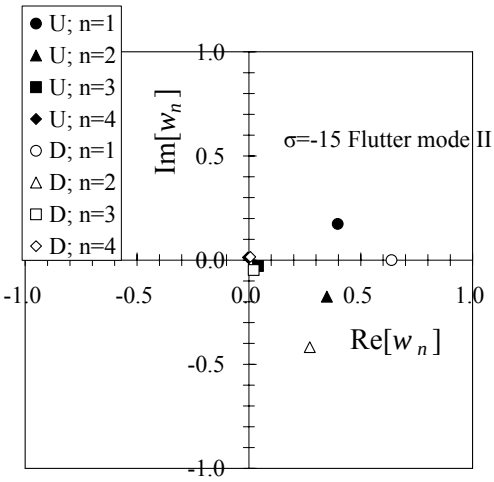

Figure 15. Complex values of the modal amplitudes of Flutter mode II at $\sigma = -15$. Configuration 1.

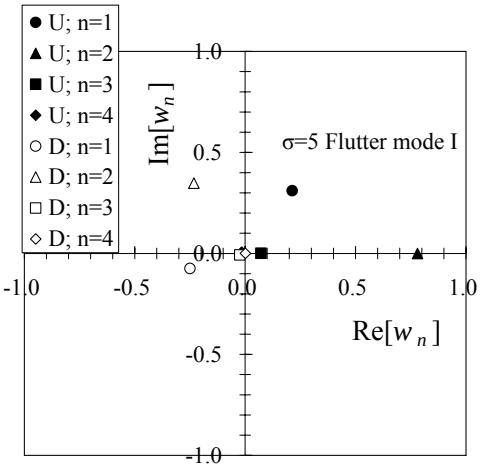

Figure 16. Complex values of the modal amplitudes of Flutter mode I at $\sigma = 5$. Configuration 1.

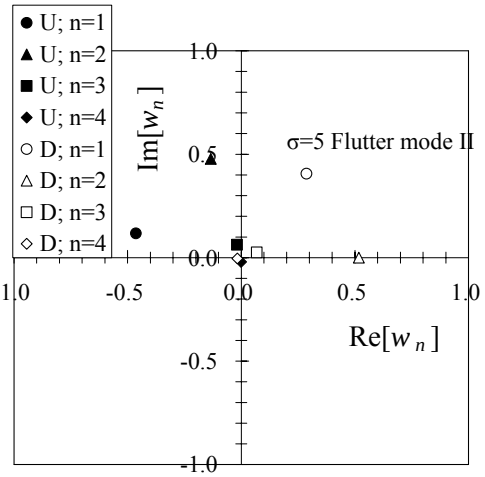

Figure 17. Complex values of the modal amplitudes of Flutter mode II at $\sigma = 5$. Configuration 1.

4. Conclusions

To investigate the effect of the aerodynamic coupling among blade rows upon the blade row flutter conditions, the flutter analyses for a model composed of rotor/stator/rotor cascades, in which the blades of the two rotor cascades are vibrating, has been conducted. From numerical studies the following conclusions are drawn.

(i) The flutter mode of an isolated blade row branches into two flutter modes, because of the aerodynamic coupling between the blade rows.

(ii) The flutter velocity is reduced by the aerodynamic coupling between the blade rows, i.e. the risk of the flutter occurrence is enhanced by the aerodynamic coupling between the blade rows.

(iii) The flutter modes are mainly composed of the first bending mode and first torsional mode.

(iv) The risk of flutter occurrence is reduced by a difference in the aeroelastic properties between the blade rows.

References

1) Hall, K. C., and Silkowski, P. D.: The Influence of Neighboring Blade Rows on the Unsteady Aerodynamic Response of Cascades, *ASME Journal of Turbomachinery*, **119**, 1997, pp.85-93.
2) Hall, K. C., and Erici, K.: R. J.: Multistage Coupling for Unsteady Flows in Turbomachinery, *AIAA Journal*, **43**, 2005, pp. 624-632.
3) Ekici, K., Voytovych, D. M., and Hall, K. C.: Time-Linearized Navier-Stokes Analysis of Flutter in Multistage Turbomachines, 43rd AIAA Aerospace Science Meeting and Exhibit, Paper 2005-0836, Reno, NV, (January 2005), 2005.
4) Ekici, K. and Hall, K. C.: Nonlinear Analysis of Unsteady Flows in Multistage Turbomachines

Using the Harmonic Balance Technique, 44 th AIAA Aerospace Science Meeting and Exhibit, Paper 2006-0422, Reno, NV, (January 2006), 2006.

5) Namba, M. and Nishino, R.: Unsteady Aerodynamic Response of Oscillating Contra-Rotating Annular Cascades Part I: Description of Modal and Mathematical Formulations, *Transaction of the Japan Society for Aeronautical and Space Sciences,* **49**, 2006, pp.175-180.
6) Nishino, R. and Namba, M.: Unsteady Aerodynamic Response of Oscillating Contra-Rotating Annular Cascades Part II: Numerical Study, *Transaction of the Japan Society for Aeronautical and Space Sciences,* **49**, 2006, pp.181-186.
7) Namba, M. and Nishino, R.: Flutter Analysis of Contra-Rotating Blade Rows, *AIAA J.*, **44**, 2006, pp.2612-2620.
8) Namba, M., Nishino, R., and Nakagawa, H.: Unsteady Aerodynamic Force on Oscillating Blades under Interaction of Three Bladerows, *Turbomachines: Aeroelasticity, Aeroacoustics and Unsteady Aerodynamics,* edited by V.A. Skibin, V.E. Saren, N.M. Savin and S.M. Frolov, Torus Press Ltd., Moscow, 2006, pp.143-154.